A new pedestrian recognition system based on edge detection and different census transform features under weather conditions

Mohammed Razzok[1], Abdelmajid Badri[1], Ilham EL Mourabit[1], Yassine Ruichek[2], Aïcha Sahel[1]

[1]Laboratory of Electronics, Energy, Automation, and Information Processing, Faculty of Sciences and Techniques Mohammedia,
University Hassan II Casablanca, Mohammedia, Morocco
[2]Laboratory CIAD, University Burgundy Franche-Comté, Belfort, France

ABSTRACT

Pedestrian detection has so far achieved great success in normal illumination, while pedestrians captured in extreme weather are often ignored. This paper investigates the importance of studying the effects of weather conditions on the recognition task, such as blurring and low contrast. Many image restoration techniques have recently been proposed, but are still insufficient to remove weather effects from images. We present our strong new pedestrian recognition system against climate situations, which is based on locating contours cues by applying multiple edge filters and extracting multiple features from images such as census transform (CT), modified census transform (MCT), and local gradient pattern (LGP) without performing any image restoration algorithm. The next stage involves finding the most discriminative characteristics using feature selection (FS) techniques. Finally, we use the final feature vector as an input to a radial basis function-based support vector machine classifier (RbfSVM) for pedestrian recognition. Experiments are performed on the daimler pedestrian classification benchmark dataset. Results show that the area under the curve (AUC) and the detection rate of our model are less affected by weather conditions compared to other common models like histogram of oriented gradients (HOG) and gabor filter bank (GFB) detectors.

This is an open access article under the CC BY-SA license.

Corresponding Author:

Mohammed Razzok
Laboratory of Electronics, Energy, Automation, and Information Processing, Faculty of Sciences and Techniques Mohammedia, University Hassan II Casablanca
Mohammedia, Morocco
Email: mohammedrazzok@gmail.com

1. INTRODUCTION

Traffic accidents in Morocco cause more than 4,000 deaths each year, 25% are pedestrians. Hence, in the last few years, the considerable interest in building pedestrian detection systems has been very active to improve traffic safety by providing drivers some information concerning their environment, any potential hazard, and performing counteractive measures in dangerous situations. Two of the most significant tasks are the recognition and localization of pedestrians in front of a vehicle.

The pedestrian detection task is particularly difficult for several reasons. For the most part, there is a wide range of possible pedestrian appearances due to changing articulated poses, clothing, lighting conditions, and cluttered backgrounds. In addition, detecting pedestrians can be more difficult with poor visibility due to the presence of fog or mist in the atmosphere. Images taken under such bad weather

conditions are subject to degradation and extreme loss of contrast. To obtain the image with good visibility from the original bad one, many researchers try to solve the problem with other additional information or only the degradation image [1]–[4].

The main work of this paper is to develop a strong pedestrian recognition system against weather conditions without applying any image restoration technique. Object contours contain a rich source of information for the discernment of shape and for the detection of pedestrians [5]. Contour cues can be estimated using multiple image processing techniques such as edge detection [6] and image segmentation [7]–[10]. Our new proposed detection framework focuses on locating contours cues by applying different edge filters on images and extracting features using different descriptors such as: census transform (CT) [11], modified census transform (MCT) [12] and local gradient pattern (LGP) [13], which can characterize critical contour information for pedestrian detection [5]. Our objectives are to show that the critical information in our proposed features can lead to efficient detection against weather effects and to prove the importance of using degradation data for model evaluation.

The rest of this paper is organized: section 2 defines the materials and methods we will address. Section 3 introduces our proposed recognition models. After presenting and discussing our test results in section 4, we conclude in section 5.

2.   MATERIALS AND METHODS
2.1. Image degradation
The degradation of images by fog and mist is a common problem that poses safety and efficiency issues to all transportation systems. In the atmospheric propagation studies, distributions of particles such as cloud, fog, haze, and mist are all known as atmospheric aerosols. The effects of such aerosols are the following: i) contrast degradation is due to the attenuation of the light caused by a cloud of solid or liquid particles in the air and/or the dispersion of some direct light flux toward the camera; ii) blurring can be caused by many factors such as long-term atmospheric turbulence, defocusing, and movement during the capture process, and iii) noise is a random variation of brightness or color information in images that comes from sensors like thermal or electrical signals and environmental conditions such as rain and snow.

2.2. Edge detection
Edge detection is a regular first step in extracting information from images. It continues to be an active area of research due to its importance in reducing the data to be processed and filtering out information that may be considered less important while conserving the important structural characteristics of an image. In edge detection, we locate the boundaries or edges of objects in an image, by determining where the brightness of the image varies significantly. Edge detectors use typically two convolution masks, one calculating gradient in the x-direction, and another calculating gradient in the y-direction. This operation can be described by (1):

$$G_x(i,j) = mask_x * I(i,j), G_y(i,j) = mask_y * I(i,j) \qquad (1)$$

where $I(i,j)$ is indicating some neighborhood of pixel (i,j) of the input image, and $*$ denotes convolution. The gradient magnitude is estimated by combining the two individual images G_x and G_y using the approximation equation $G_x = \sqrt{G_x{}^2 + G_y{}^2}$ and rescaled to [0.255] by (2):

$$G_{changed} = 255.\frac{G - G_{min}}{G_{max} - G_{min}} \qquad (2)$$

Edge filters used in this paper are the following:
a)   Sobel: uses two 3 by 3 kernels to detect gradients in the horizontal and the vertical directions.

$$mask_x = \begin{bmatrix} -1 & 0 & +1 \\ -2 & 0 & +2 \\ -1 & 0 & +1 \end{bmatrix}, mask_y = \begin{bmatrix} -1 & -2 & -1 \\ 0 & 0 & 0 \\ +1 & +2 & +1 \end{bmatrix} \qquad (3)$$

b)   Roberts: uses two 2 by 2 kernels to measure gradients in opposing diagonal directions.

$$mask_x = \begin{bmatrix} +1 & 0 \\ 0 & -1 \end{bmatrix}, mask_y = \begin{bmatrix} 0 & +1 \\ -1 & 0 \end{bmatrix} \qquad (4)$$

c)   Prewitt: uses two 3 by 3 kernels to measure horizontal and vertical gradients.

$$mask_x = \begin{bmatrix} -1 & 0 & +1 \\ -1 & 0 & +1 \\ -1 & 0 & +1 \end{bmatrix}, mask_y = \begin{bmatrix} -1 & -1 & -1 \\ 0 & 0 & 0 \\ +1 & +1 & +1 \end{bmatrix} \qquad (5)$$

d)   Local variance: local statistics can establish the gradient of the image. The local variance can be used to produce the edge map. Our modified edge detection based on local variance can be outlined:
−   Read the image as grayscale
−   Define a window size (3,3)

$$k = \frac{1}{9} \cdot \begin{bmatrix} 1 & 1 & 1 \\ 1 & 1 & 1 \\ 1 & 1 & 1 \end{bmatrix}$$

−   Calculate the local variance $L_{var} = k * (I^2) - (k * I)^2$, where * denotes convolution
−   Compute the global median of the local variance image L_{var}
−   Set local variance to 255 if it is strictly less than the global median else set it to zero

2.3. Image descriptors
Image descriptors are the topic of image processing, which require the use of algorithms to compute and extract certain attributes to represent the image. Image descriptors, for example, describe basic characteristics such as shape, color, texture, or motion. Image descriptors used in this paper are the following:

2.3.1. Census transform (CT)
CT is a non-parametric local transform that was first proposed by Zabih and Woodfill [11]. CT compares the intensity value of the center pixel with its eight neighboring pixels to obtain an 8 binary string, which is converted into a decimal number between 0 and 255. The CT value for the pixel (x_c, y_c) is given by (6):

$$CT(x_c, y_c) = \sum_{p=0}^{7} s(i_p - i_c) \cdot 2^p, \ s(x) = \begin{cases} 1, & x \geq 0 \\ 0, & \text{otherwise} \end{cases} \qquad (6)$$

where i_c is the gray value of the central pixel, i_p is the value of its neighbors. The most important properties of CT are its tolerance against illumination changes, gamma variations, and computational simplicity.

2.3.2. Modified census transform (MCT)
MCT was proposed by Froba and Ernst [12] in the context of texture analysis. MCT is a variation of CT where the measure incorporates the mean intensity of the neighborhood (including the center pixel). Let the mean intensity be denoted as $\bar{i}_c$. Therefore it can be calculated as:

$$\bar{i}_c = \frac{1}{9} \sum_{n=0}^{8} i_p \qquad (7)$$

Then the MCT value for the pixel (x_c, y_c) is given by (8):

$$MCT(x_c, y_c) = \sum_{p=0}^{8} s(i_p - \bar{i}_c) \cdot 2^p, \ s(x) = \begin{cases} 1, & x \geq 0 \\ 0, & \text{otherwise} \end{cases} \qquad (8)$$

2.3.3. Local gradient pattern (LGP)
LGP is an amelioration over the traditional MCT, proposed by Jun and Kim[13]. LGP emphasizes the local variation in the neighborhood by incorporating the intensity gradient profile of the neighborhood in the measure. The average gradient is given by (9):

$$\bar{g} = \frac{1}{8} \sum_{p=0}^{7} g_p, \ g_p = |i_p - i_c| \qquad (9)$$

Then the LGP value for the pixel (x_c, y_c) is given by (10):

$$LGP(x_c, y_c) = \sum_{p=0}^{7} s(g_p - \bar{g}) \cdot 2^p, \quad s(x) = \begin{cases} 1, & x \geq 0 \\ 0, & \text{otherwise} \end{cases} \qquad (10)$$

2.4. Feature selection (FS)

In real-world concept learning problems, data representation frequently employs a large number of features, only a subset of which may be related to the target concept. FS methods [14], [15] involve selecting input variables that have the strongest correlation with the target variable and removing irrelevant, insignificant, and unimportant features to achieve higher accuracy. These are the main reasons to use FS: i) Simplifying data visualization and data understanding, ii) Reducing storage requirements, iii) Improving the accuracy of classifiers, iv) Decreasing over-fitting, and v) Reducing training and prediction time of classifiers

There are many FS techniques, we are particularly interested in the SelectFromModel meta transformer, which is from sklearn.feature_selection module [16], it is a function that can be used with any classifier having feature_importances_ attribute after fitting. The features are considered irrelevant and excluded if the corresponding feature importances values are below the threshold parameter provided. In this paper, we use linear support vector machine (SVM) [17] to compute feature_importances_, which can then be used to discard irrelevant features by using the SelectFromModel function.

3.   PROPOSED RECOGNITION MODELS

In order to study the importance of using degradation data for model evaluation, we propose two models shown in Figures 1 and 2. The first method is based on applying CT descriptor on the input image and extracting histograms from the resulting image by dividing it into 27 (9,3) blocks with size 6×4. Histograms for all blocks are concatenated. Final feature vectors are normalized (L2) and trained using radial basis function-based support vector machine classifier (RbfSVM) [17]. The second method is the same as the first only we use CT based on uniform pattern (CTU) instead of CT descriptor. Patterns with most two circular 0-1 and 1-0 transitions are referred to as uniform. For example, patterns 11111111, 00000000, 00011100, and 11111011 are uniform, and patterns 01010000, 01001110, or 10101100 are not uniform. When we extract histograms, each uniform pattern has its own bin, and all non-uniform patterns are assigned to a single bin.
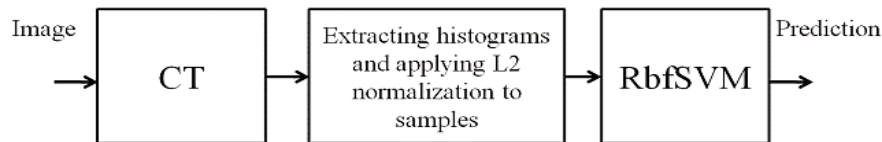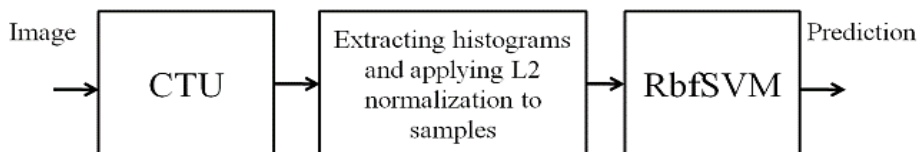

Figure 1. CT+RbfSVM model

Figure 2. CTU+RbfSVM model

Another important objective is to reduce the effects of degradation on the recognition rate by proposing a new method based on applying different processing techniques to images especially edge filters and extracting CT-MCT-LGP features. Local histograms have been collected by dividing every image into 27 (9,3) blocks with size 6×4. Histograms for all blocks are concatenated and all variables are scaled to [0,1] for several reasons, such as applying different descriptors, using distance-based classifier (SVM), and before measuring variables importance, so that all the features contribute equally to the results. We use the FS technique to reduce the length of the final feature vector from 26,055 to 9,878. Final feature vectors are classified using the RbfSVM classifier. The architecture of our model is described in Figure 3. Using uniform patterns, the length of CT and LGP feature vectors for a single block is reduced from 256 to 59, and from 512 to 75 for the MCT feature vector. In our work, we are using uniform patterns only to reduce the length of feature vectors (histograms) and to increase the efficiency of classifiers in terms of speed.
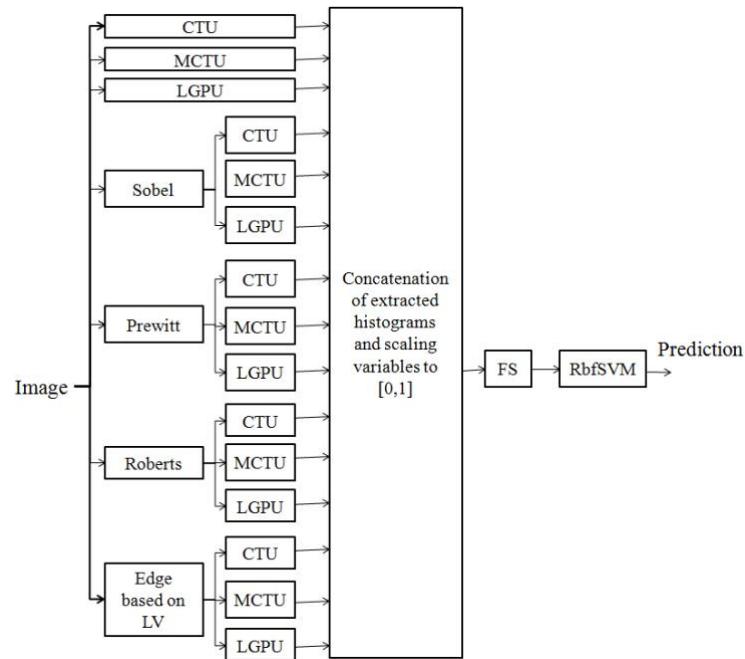
Figure 3. Proposed model against weather conditions

4. RESULTS AND DISCUSSION

For our experiments, we use the Daimler mono pedestrian classification benchmark dataset [18] to determine the efficacy of different proposed methods. The classification dataset consists of five folders, three folders for training, and two folders for testing (T1, T2). Each folder contains a total of 4,800 pedestrian and 5,000 non-pedestrian samples taken from video images and scaled to 18×36 common size.

In our study, we use three different types of data:
− Normal-data: same as the original dataset.
− Blurred-data: we simulate the blurred effects on images by applying a Gaussian filter (3,3) (Kernel generated by cv2.GaussianBlur(image,(3,3),0) function [19]).
− Contrast-data: we simulate the contrast degradation by multiplying image pixels value by a factor of (0.3).

During the model-building process, we use the k-fold cross-validation method [20]. Cross-validation techniques allows us to compare the performance of different machine learning models while selecting appropriate parameters. In our work K=3, folder 1 and folder 2 are used for training, and folder 3 is used for validation.

For model-evaluation, we use the receiver operating characteristic curve (ROC) because it indicates the true positive rate (TPR) and the false positive rate (FPR) for each threshold not like accuracy just for threshold=0.5. We picked the best possible TPR and FPR (noted x in ROC curve) using G-mean score, and we used the area under the curve (AUC) because it tells how much our models are capable of distinguishing between classes (pos/neg samples), it is also used as a summary of the ROC curve. Models are executed on Windows7 OS and python integrated development environment (IDLE) v2.7.15 using a computer with Intel Xeon CPU E3-1226 v3 Quard-core 3.3 GHz and 12Go of RAM.

In order to study the importance of using degradation data for model evaluation, we train our two models shown in Figures 1 and 2. The results are presented in Figures 4 and 5, Tables 1 and 2 respectively. CT and CTU models show comparable results (AUC, TPR, FPR) for normal images but large differences for degraded images shown in Table 1 and Table 2, implying that model evaluation should include both normal and degraded images.

To demonstrate the effectiveness of our proposed model as seen in Figure 3 against weather degradation, we compared it with two common significant methods. The first method proposed by Dalal and Triggs [21] based on histogram of oriented gradients (HOG) features inspired on scale invariant feature transform (SIFT) [22] and SVM learning machine. HOG characteristics model the form and appearance using normalized histograms of the image gradient orientation. The idea is to divide the image into small regions called cells. A cell is described as a histogram of its local gradients binned by orientation and weighted by magnitude. These cells are clustered together in larger areas called blocks. A block is defined as

a feature vector generated by concatenated and normalized histograms of its cells. The feature vectors for all blocks are concatenated to produce the final feature vector. All final feature vectors are classified using a linear SVM.
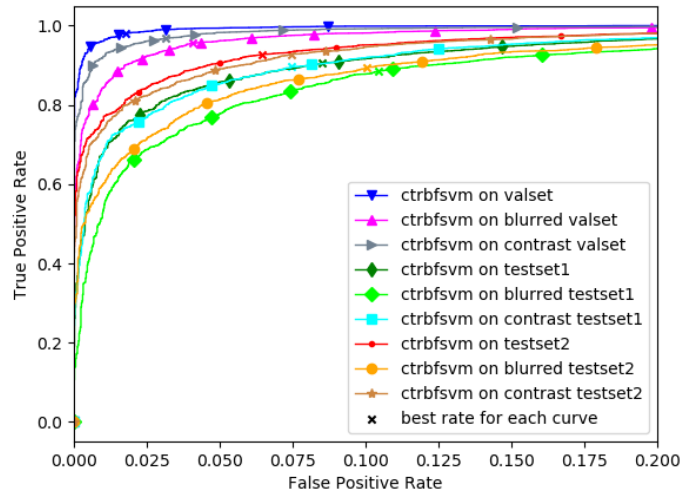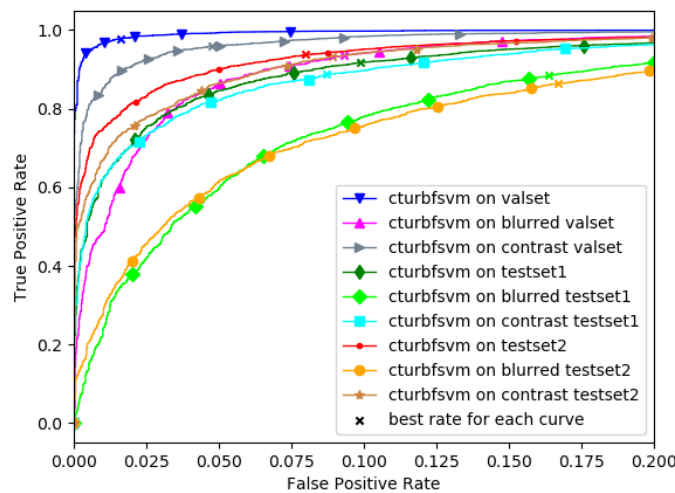

Figure 4. CT+ RbfSVM ROC

Figure 5. CTU+RbfSVM ROC

Table 1. CT+RbfSVM performance				
Data	Degradation effects	AUC	TPR(%)	FPR(%)
Val	None	0.998366	98.0833	1.7800
	Blurred	0.991940	95.5625	4.0600
	Contrast	0.995720	96.8333	3.1400
Test1	None	0.971521	90.5	8.5
	Blurred	0.955368	88.6042	10.46
	Contrast	0.972525	89.5625	7.46
Test2	None	0.982416	92.7292	6.44
	Blurred	0.963774	89.5208	10.04
	Contrast	0.980687	92.8125	7.46

Table 2. CTU+RbfSVM performance				
Data	Degradation effects	AUC	TPR(%)	FPR(%)
Val	None	0.998315	97.8750	1.6
	Blurred	0.974226	93.6250	9.3200
	Contrast	0.991852	95.9583	4.74
Test1	None	0.970978	91.8125	9.86
	Blurred	0.930177	88.5	16.38
	Contrast	0.967501	88.75	8.7
Test2	None	98.2003	93.7917	8
	Blurred	92.6765	86.4375	16.68
	Contrast	97.7381	93.25	8.9

From our training results, it appears that fine binning (9 orientation) and large scale features (blocks of 2×2 cells of 2×2 pixels) are the best parameters for the Daimler dataset. Block histograms are normalized

using the L1 technique and final feature vectors are normalized using the L2 technique. For better performance, we train final feature vectors using RbfSVM instead of linear SVM because of the small size of images on the dataset.

The second method [23] is based on extracting features by applying gabor filter bank (GFB) and linear SVM for classification. Our best modified feature extractor that we can achieve for our dataset consists of three steps: convolution of the input image with multiple gabor filters, splitting the image into sub-images, and calculation of statistical feature values. We apply 120 filters to the input image, the size of each kernel is 16×16. Gabor filters are generated by varying sigma to 0.001, 1.62377674e-03, 2.63665090e-03, 4.28133240e-03, 6.95192796e-03, 1.12883789e-02, 1.83298071e-02, 2.97635144e-02, 4.83293024e-02, 7.84759970e-02, 1.27427499e-01, 2.06913808e-01, 3.35981829e-01, 5.45559478e-01, 8.85866790e-01, 1.43844989, 2.33572147, 3.79269019, 6.15848211, 10 (generated by numpy.logspace(-3,1,num=20) function [24], [25]) and theta (0 to $5. \pi/6$ by $\pi/6$ step), lambda is set to 1, and gamma to 0.001.

The result 18×36 image is divided into 27 (9,3) sub-images with size 6×4. For each sub-image, three statistical features (mean, standard deviation, and skewness) are calculated. Consequently, the dimension of the feature vector is 9720 (20×6×27×3=9720). All variables of features vectors are scaled to [0,1] due to the different wide range of features (mean, standard deviation, and skewness), then we train finally vectors by using RbfSVM classifier. Figure 6, Table 3, Figure 7, Table 4, Figure 8, and Table 5 show the weather effects on our proposed model, HOG and GFB detectors respectively.
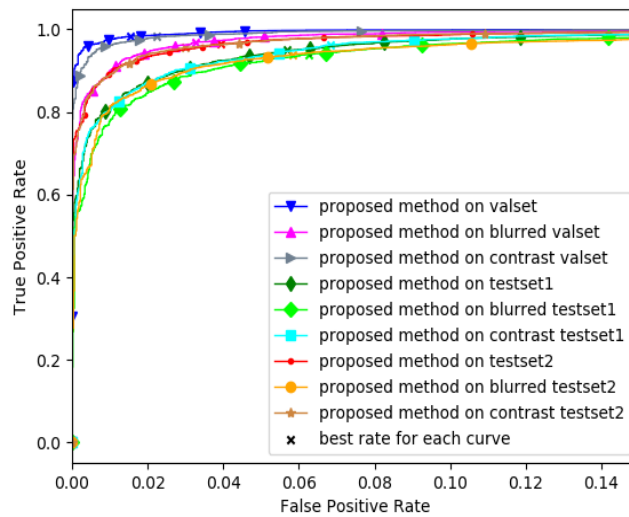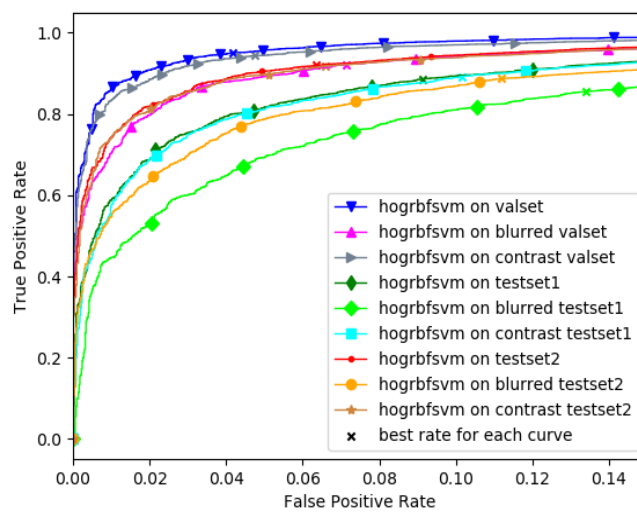

Figure 6. Proposed method ROC

Figure 7. HOG+RbfSVM ROC

Table 3. Proposed method performance

Data	Degradation effects	AUC	TPR(%)	FPR(%)
Val	None	0.998877	98.3542	1.54
	Blurred	0.995393	96.8958	3.28
	Contrast	0.998095	98.1875	2.24
Test1	None	0.989015	94.9375	5.7
	Blurred	0.985071	94	6.26
	Contrast	0.989094	96.2708	6.82
Test2	None	0.994067	96.5208	3.92
	Blurred	0.985453	93.9792	5.84
	Contrast	0.994187	95.6042	2.98

Table 4. HOG+RbfSVM performance

Data	Degradation effects	AUC	TPR(%)	FPR(%)
Val	None	0.991113	95.0208	4.16
	Blurred	0.978146	92.2292	7.14
	Contrast	0.988583	94.3750	4.76
Test1	None	0.964186	88.6458	9.14
	Blurred	0.938031	85.5833	13.4
	Contrast	0.962219	89.25	10.16
Test2	None	0.979831	92.0208	6.34
	Blurred	0.954836	88.6875	11.18
	Contrast	0.978818	91.7917	6.58

Our comparison reveals a number of interesting points, every image recognition technique has its own characteristics. The recognition rate of the GFB model gets influenced by contrast more than blur degradation. On the other hand, the HOG model is affected by blur more than contrast degradation, see Figure 7, Table 4, Figure 8, and Table 5. As a result, choosing appropriate image restoration techniques for better model performance depends on how models react to degradation effects.
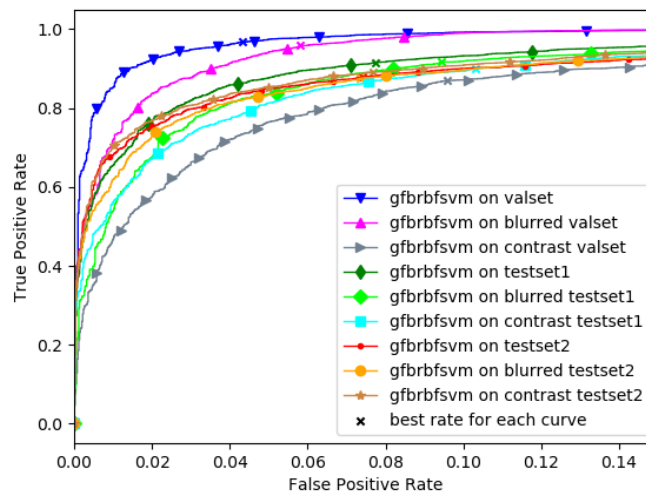
Figure 8. GFB+RbfSVM ROC

Table5. GFB+RbfSVM performance

Data	Degradation effects	AUC	TPR(%)	FPR(%)
Val	None	0.993526	96.7292	4.32
	Blurred	0.988470	95.8333	5.82
	Contrast	0.954620	87	9.6
Test1	None	0.975297	91.5833	7.74
	Blurred	0.967258	91.6667	9.44
	Contrast	0.961953	89.9792	10.3
Test2	None	0.959085	87.9792	7.4
	Blurred	0.960343	87.5833	7.36
	Contrast	0.965632	89.1458	7.68

For validation samples, AUC of our proposed method against contrast degradation decreases by 0.08%, HOG detector decreases by 0.26%, gabor detector decreases by 3.92%. For blurred effects, AUC of our proposed method decreases by 0.35%, HOG detector decreases by 1.31% and Gabor detector decreases by 0.51%. The execution time prediction of our models can be decomposed into two main elements: the extracting time of features of the input image and the prediction time of features by the classifier. Our proposed method against weather conditions requires around 0.2s to predict the input image, 0.04s for HOG detector, and 0.8s for GFB detector. We can conclude that the time prediction might seem a priori a weakness of our model due to the computational time of the multiple filters and descriptors applied but our model has the advantage of being less affected by degradation effects compared to other common models HOG and GFB detectors. Figure 9 shows some images from the T1 folder were resisted by our proposed model to weather conditions but not to (contrast or blurred) conditions by others models (HOG and GFB). Another important point to add is that low-resolution resized images lead to the loss of critical information. As a result, models trained with small-size images and tested on large images may cause false-positive predictions.
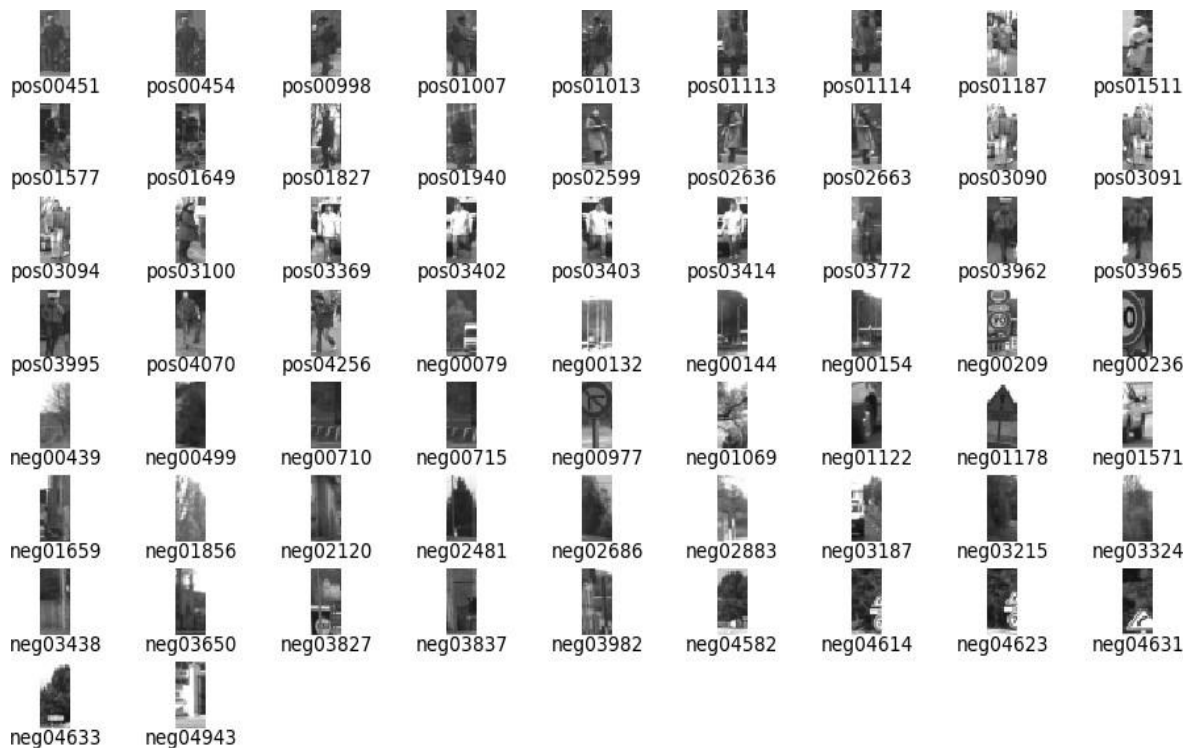
Figure 9. Images from the T1 folder were resisted by our proposed model to weather conditions but not to (contrast or blurred) conditions by other models (HOG and GFB)

5.   CONCLUSION

In this paper, different types of pedestrian recognition systems are implemented and the results are compared by using the performance parameters AUC, TPR, FPR. Our proposed method based on extracting CT-MCT-LGP features from images by applying multiple edge filters shows good performance in terms of recognition rate and resistance to weather conditions compared to other common models like HOG and GFB detectors. The results are very promising, but there are still some perspectives for our future research, the first is the development of a pedestrian detection system using cascading classifiers and parallel computing technology (GPU acceleration) to achieve both a high detection rate and real-time detection. Next, we intend to use infrared (IR) cameras to detect pedestrians at night. Finally, up-scale low-resolution training and testing images to improve image details and increase the detection rate.

REFERENCES

[1]   C. Dai, M. Lin, X. Wu, and D. Zhang, "Single hazy image restoration using robust atmospheric scattering model," *Signal Processing*, vol. 166, Jan. 2020, doi: 10.1016/j.sigpro.2019.107257.

[2]   M. Ju, C. Ding, W. Ren, Y. Yang, D. Zhang, and Y. J. Guo, "IDE: image dehazing and exposure using an enhanced atmospherics scattering model," *IEEE Trans. Image Process.*, vol. 30, pp. 2180–2192, 2021, doi: 10.1109/TIP.2021.3050643.

[3]   S. Hong, M. Kim, and M. G. Kang, "Single image dehazing via atmospheric scattering model-based image fusion," *Signal Processing*, vol. 178, Jan. 2021, doi: 10.1016/j.sigpro.2020.107798.

[4]   Y. -J. Zhang, "Image repair and recovery," in *Handbook of Image Engineering*, Singapore: Springer Singapore, 2021, pp. 605–621.

[5]   J. Wu, C. Geyer, and J. M. Rehg, "Real-time human detection using contour cues," in *2011 IEEE International Conference on Robotics and Automation*, May 2011, pp. 860–867, doi: 10.1109/ICRA.2011.5980437.

[6]   S. Kumar, A. K. Upadhyay, P. Dubey, and S. Varshney, "Comparative analysis for edge detection techniques," in *2021 International Conference on Computing, Communication, and Intelligent Systems (ICCCIS)*, Feb. 2021, pp. 675–681, doi: 10.1109/ICCCIS51004.2021.9397225.

[7]   A. W. Rosyadi, and N. Suciati, "Image segmentation using transition region and K-means clustering," *IAENG Int. J. Comput. Sci.*, vol. 47, no. 1, pp. 47–55, 2020.

[8]   W. Ding, Y. Zhao, and R. Zhang, "An adaptive multi-threshold segmentation algorithm for complex images under unstable imaging environment," *Int. J. Comput. Appl. Technol.*, vol. 61, no. 4, pp. 265–272, 2019, doi: 10.1504/IJCAT.2019.103295.

[9]   H. Zhang, S. Wang, X. Xu, T. W. S. Chow, and Q. M. J. Wu, "Tree2Vector: learning a vectorial representation for tree-structured data," *IEEE Trans. Neural Networks Learn. Syst.*, vol. 29, no. 11, pp. 5304–5318, Nov. 2018, doi: 10.1109/TNNLS.2018.2797060.

[10] C. Tan, Y. Sun, G. Li, B. Tao, S. Xu, and F. Zeng, "Image segmentation technology based on genetic algorithm," in *Proceedings of the 2019 3rd International Conference on Digital Signal Processing - ICDSP 2019*, 2019, pp. 27–31, doi: 10.1145/3316551.3318229.

[11] R. Zabih and J. Woodfill, "Non-parametric local transforms for computing visual correspondence," in *Computer Vision*, Springer Berlin Heidelberg, 1994, pp. 151–158.

[12] B. Froba and A. Ernst, "Face detection with the modified census transform," in *Sixth IEEE International Conference on Automatic Face and Gesture Recognition, 2004. Proceedings.*, 2004, pp. 91–96, doi: 10.1109/AFGR.2004.1301514.

[13] B. Jun and D. Kim, "Robust face detection using local gradient patterns and evidence accumulation," *Pattern Recognit.*, vol. 45, no. 9, pp. 3304–3316, Sep. 2012, doi: 10.1016/j.patcog.2012.02.031.

[14] U. M. Khaire and R. Dhanalakshmi, "Stability of feature selection algorithm: a review," *J. King Saud Univ. - Comput. Inf. Sci.*, Jun. 2019, doi: 10.1016/j.jksuci.2019.06.012.

[15] S. Solorio-Fernández, J. A. Carrasco-Ochoa, and J. F. Martínez-Trinidad, "A review of unsupervised feature selection methods," *Artif. Intell. Rev.*, vol. 53, no. 2, pp. 907–948, Feb. 2020, doi: 10.1007/s10462-019-09682-y.

[16] M. Blondel *et al.*, "Scikit-learn: machine learning in Python," *J. Mach. Learn. Res.*, vol. 12, pp. 2825–2830, 2011.

[17] J. Cervantes, F. Garcia-Lamont, L. Rodríguez-Mazahua, and A. Lopez, "A comprehensive survey on support vector machine classification: Applications, challenges and trends," *Neurocomputing*, vol. 408, pp. 189–215, Sep. 2020, doi: 10.1016/j.neucom.2019.10.118.

[18] S. Munder and D. M. Gavrila, "An experimental study on pedestrian classification," *IEEE Trans. Pattern Anal. Mach. Intell.*, vol. 28, no. 11, pp. 1863–1868, Nov. 2006, doi: 10.1109/TPAMI.2006.217.

[19] G. Bradski and A. Kaehler, *Learning openCV*, vol. 53, no. 9. O'Reilly Media, 2008.

[20] D. Berrar, "Cross-validation," in *Encyclopedia of Bioinformatics and Computational Biology*, vol. 1–3, Elsevier, 2019, pp. 542–545.

[21] N. Dalal and B. Triggs, "Histograms of oriented gradients for human detection," in *2005 IEEE Computer Society Conference on Computer Vision and Pattern Recognition (CVPR'05)*, 2005, vol. 1, pp. 886–893, doi: 10.1109/CVPR.2005.177.

[22] M. I. Ouloul, Z. Moutakki, K. Afdel, and A. Amghar, "An efficient face recognition using SIFT descriptor in RGB-D images," *Int. J. Electr. Comput. Eng.*, vol. 5, no. 6, pp. 1227–1233, Dec. 2015, doi: 10.11591/ijece.v5i6.pp1227-1233.

[23] S. Lee, J.-W. Jang, and K.-R. Baek, "Pedestrian detection algorithm using a gabor filter bank," *J. Inst. Control. Robot. Syst.*, vol. 20, no. 9, pp. 930–935, Sep. 2014, doi: 10.5302/J.ICROS.2014.13.0020.

[24] T. E. Oliphant, *A guide to NumPy*. Trelgol Publishing, 2006.

[25] S. van der Walt, S. C. Colbert, and G. Varoquaux, "The NumPy array: a Structure for efficient numerical computation," *Comput. Sci. Eng.*, vol. 13, no. 2, pp. 22–30, Mar. 2011, doi: 10.1109/MCSE.2011.37.

BIOGRAPHIES OF AUTHORS

Mohammed Razzok received the Engineering degree in networks and telecommunications from the National School of Applied Sciences (ENSA), Oujda, Morocco, in 2017. He is currently pursuing his Ph.D. in the computer vision field at the Laboratory of Electronics, Energy, Automation and Information Processing, Faculty of Sciences and Techniques Mohammedia, University Hassan II Casablanca, Morocco. His main research is constructing and implementing on-board systems for intelligent vehicles to perform pedestrian recognition/detection, analyze pedestrian trajectories, warn the driver or initiate appropriate protective measures when detecting potentially dangerous situations. Email: mohammedrazzok@gmail.com.
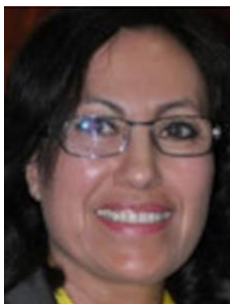
Abdelmajid Badri holds a Ph.D. in Electronics and Image Processing from the University of Poitiers, France, in 1992. In 1996, he got the diploma of authorization to manage researches at the University of Poitiers France. He is a director at the Higher School of Technology (EST), Casablanca, and he is a University Professor (PES-C) at FST Mohammedia, University Hassan II of Casablanca, Morocco where he teaches electronics, signal processing, image processing, and telecommunication. He is a member of the electronic, energy, automatic and information processing (EEA and TI) laboratory which he managed since 1996. His research focuses on communication and information technology (electronics systems, signal/image processing, and telecommunication). He is qualified by the CNU-France in the 61st section: computer engineering, automatic, and signal processing. He managed multiple doctoral theses. He is a co-author of several national and international publications and is responsible for many research projects financed by the ministry or by the industrialists. He was a member of several committees and programs of international conferences and president of three international congresses in the same domain. He is a member and co-responsible for multiple scientific associations in touch with his domain of research. Email: abdelmajid_badri@yahooo.fr.

Ilham El Mourabit holds a Ph.D. degree in Electronic Systems and Telecommunications in 2018. She is a University Professor at FST Mohammedia. She received the B.Sc. degree in Electronics and Computer Science, from the Faculty of Sciences and Technology of Mohammedia, Hassan II University Casablanca, Morocco, in 2009, and an M.Sc. degree in Electronic and Automatic Systems Engineering (telecommunication and information technologies specialty) from the same institution. Her main research areas are how to use satellite and cellular network's signals to determine the accurate position of a mobile target to perform real-time monitoring. Email: Elmourabit.ilham@gmail.com.

Yassine Ruichek (Senior Member, IEEE) holds a Ph.D degree in control and computer engineering in 1997 and the authorization to manage researches (HDR) degree in physic science from the University of Lille, France, in 2005. In 2007 he became a full professor at the University of Technology of Belfort-Montbéliard (UTBM). His research interests include computer vision, image processing and analysis, pattern recognition, data fusion, and localization, with applications in intelligent transportation systems and video surveillance. Email: yassine.ruichek@utbm.fr.

Aïcha Sahel holds a Ph.D. in Electronics and Image Processing from the University of Poitiers, France, in 1996. She is a Professor at FST Mohammedia, University Hassan II of Casablanca, Morocco, and a member of the EEA and TI laboratory. Aicha Sahel's research focuses on electronic systems, signal/image processing, and telecommunications. She co-supervises doctoral theses and co-authors of several national and international publications and is a member of multiple financed research projects. She was a member of the steering committees of three international congresses in the same field of research. Email: sahel_ai@yahoo.fr.